ORIGINAL ARTICLE

A novel methodology for predicting and identifying geometric errors of rotary axis in five-axis machine tools

Jinwei Fan[1] · Yiling Zhang[1]

Abstract

The geometric errors of rotary axes are crucial error sources of a five-axis machine tool. They directly affect the machining accuracy, and therefore become one of the most important items for accuracy design. In this paper, a prediction and identification method for the geometric errors of rotary axes on a five-axis machine tool is proposed. The prediction is realized by calculating the mapping relationship between tolerances and geometric errors of rotary axes, which is based on exploring rotary axes' motion regulation and Fourier series fitting. Then in order to figure out the practical geometric errors of rotary axes, the identifying model is established based on homogeneous transform matrix (HTM). Double ball-bar (DBB) is adopted to test error motions of rotary axes. Finally, a demonstration experiment has been conducted for verifying the effectiveness and precision of the proposed prediction model. The experimental results show that the predicting model is able to reflect the motion principle of rotary axes' kinematic errors. The SSE, which expresses residual sum of squares between estimated value and identified point, of $\varepsilon_z(c), \delta_x(c), \varepsilon_y(c), \delta_z(c), \varepsilon_x(c)$, and $\delta_y(c)$, are 7.7716×10^{-11}, 1.2064×10^{-4}, 2.7838×10^{-10}, 2.9639×10^{-7}, 1.8966×10^{-10}, and 2.7838×10^{-10}, respectively. And R^2, who represent fitting equation's coefficient of determination, of abovementioned geometric errors, are 0.8978, 0.9876, 0.9978, 0.9453, 0.9985, and 0.9978, respectively. The computing results show that two kinds of curves are basically coincide, and the proposed method is proven to be feasibility.

Keywords Rotary axis · Tolerance · Geometric error prediction · DBB test

1 Introduction

With the increasing requirements for the complicated [1] and strict quality required work-piece [2] with sculptured or free-form surfaces [3, 4], five-axis machine tools are indispensable in the modern manufacturing industry [5]. Two additional rotary axes are applied for controlling orientation of the cutting tool [6, 7], and continuously adjusted the cutter's effective curvature [8]. Compared with three-axis machine tools, there are more advantages in five-axis machine tools, such as higher machining efficiency [9], lower cutting time [10], less work-piece set-up time [11], and higher productivity [5]. However, 80% of total error sources are introduced for the additional rotary axes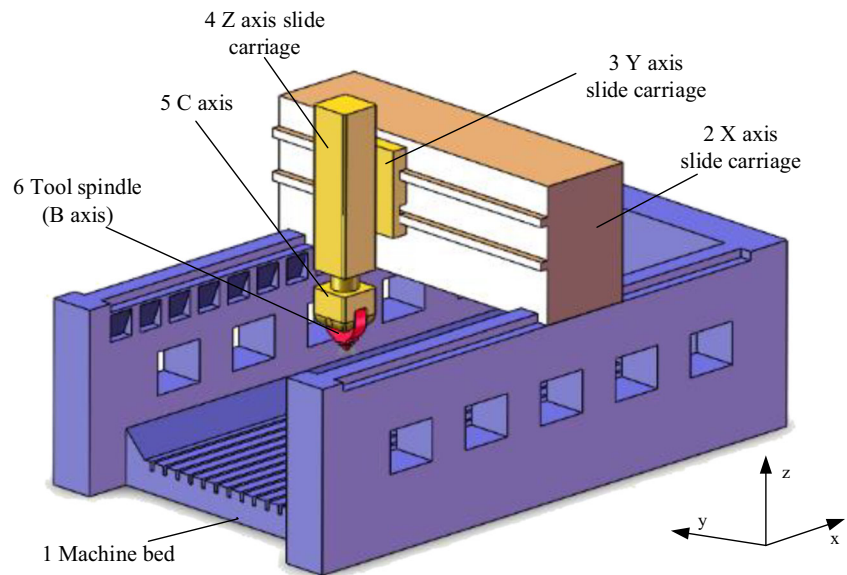 [12], and bring about flaws and defects in finished work-piece. Hence, researching on geometric errors of rotary axes is significant to improve machining accuracy of five-axis machine tools [13].

Over the past few decades, the error measurement researches have been refined into the error parameters of the movement axis, which makes it possible to calculate the volumetric error of any position and orientation among the workspace of machine tools [14]. DBB is a mature measuring instrument [15] and preferred to be utilized to test volumetric errors of rotary axes [16–18] in order to identify the error parameters. Zhang et al. [19] designed two DBB-measuring paths which are in different horizontal planes for decoupling geometric errors of five-axis machine tools' rotary table. Lee et al. [6] simplified the measurement procedures of DBB by using a single controlled axis during the measurement. Xiang et al. [15] adopted three measuring patterns to obtain a circular trajectory which is generated by the linkage of two rotary axes for identifying the linkage errors of a five-axis machine tool. Lei et al. [12] developed a general ball bar test method for inspecting dynamic errors of rotary axes in five-axis machine tools. Jiang et al. [11] presented a new DBB measurement

✉ Yiling Zhang
s201701041@emails.bjut.edu.cn

[1] College of Mechanical Engineering and Applied Electronics Technology, Beijing University of Technology, Beijing 100124, People's Republic of China

Fig. 1 Structure of gantry-type milling machine tool

4 Z axis slide carriage

3 Y axis slide carriage

5 C axis

2 X axis slide carriage

6 Tool spindle (B axis)

1 Machine bed

procedure which avoids coupling among axes and is universal to all types of five-axis machine tools. Chen et al. [20] proposed a circular fitting method to identify the five-axis machine tool's linkage errors by DBB, measured the integrated errors of a tilt table's sensitive direction. Jiang et al. [21] presented a comprehensive geometric model which could depict universal kinematic errors of universal machine tools without Abbe errors [22]. Fu et al. [23] developed a systematic accuracy enhancement approach of five-axis machine tools based on differential motion matrix. Lu et al. [24] presented a new two-dimensional method which could analyze spindle radial error motion measurement. In order to improve machining accuracy of non-orthogonal five-axis machine tools, Wu et al. [25] established an integrated geometric error modeling method based on the relative motion constraint equations, and developed an effective iterative compensation method. Liu et al. [18] proposed a volumetric accuracy enhancement method of rotary axes based on screw theory, and established the geometric error model via constructing equivalent rotary axis.
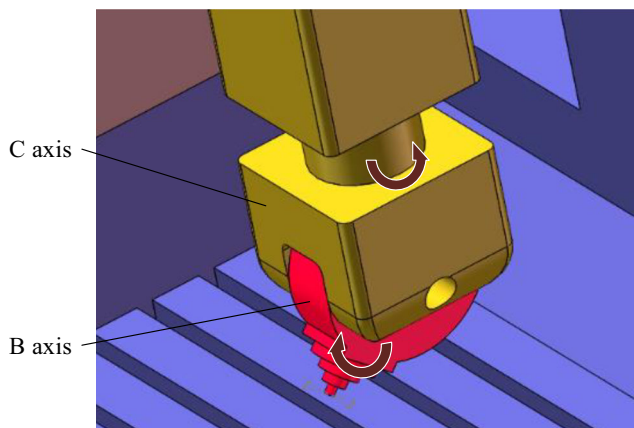
As can be observed in the abovementioned researches, the present work about rotary axis is aiming at geometric errors modeling, identification, and compensation; the aspect in predicting geometric errors of rotary axes is ignored. Geometric errors, which provide guidance for the accuracy design of new machine tools during the design process [26], are one of the most important parameters of accuracy design. In the initial design stage of machine tools, only the information of tolerances of rotary axes are known, while geometric errors are unknown, since geometric errors are parameters generated after assembly of machine tools [7, 25, 27, 28]. Nowadays, the way that designers and engineers obtain geometric errors is just by making use of design experiences [26] without quantify, which cause some inherent and unavoidable defects of the machine tools. Therefore, an effective approach
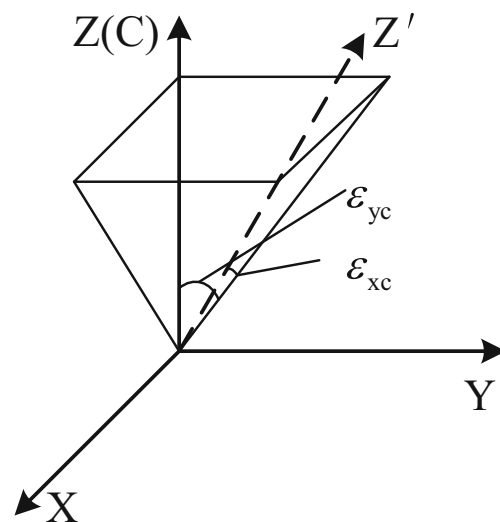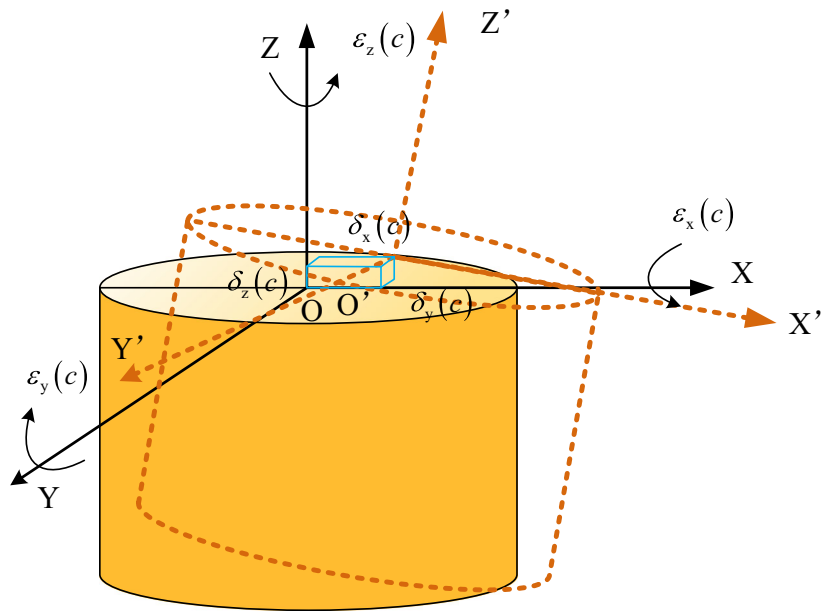
Fig. 2 Rotary axes of gantry-type milling machine tool

C axis

B axis

Fig. 3 Squareness errors of C-axis

$Z(C)$

Z'

ε_{yc}

ε_{xc}

Y

X

Fig. 4 The six basic error components of C-axis

to the prediction and calibration of geometric errors during the design stage of machine tools is significant in practice.

There are several researches have predicted geometric errors of translational axes. Wu et al. [27] proposed a prediction and compensation method of integrated geometric errors for translational axes in one type five-axis machine tools to enhance positioning accuracy. Ekinci et al. [29] considered machine errors at more fundamental levels and presented a method of expressing the geometric profile errors of guideways by Fourier series. Based on Ekinci's theory, Fan et al. [26] have worked out the mapping relationship between geometric profile errors of machine tools' guideways and the tolerances, demonstrated that in design stage geometric errors are possible to be known parameters. However, unlike linear axes, the motion of rotary axes is cyclic [1]; there exist fundamental differences in internal structure between rotary axes and translational axes; the theoretical models of two kinds of axes are diverse. So the proposed method of predicting geometric errors to multi-axis machine tools' linear axes is rarely available for rotary axes. To sum up, it is necessary to develop a predicting method which is aiming at geometric errors of five-axis machine tools' rotary axes.

In this study, a systematic approach to predict geometric errors of rotary axes in five-axis machine tools based on tolerances is developed. The ties between geometric errors and tolerances are geometric profile errors. Truncated Fourier series is utilized to represent rotary axis error motion, which is cyclic in nature over 360-degree repeating travel. After that, to verify the effectiveness of presented theory, a geometric error identification model of rotary axes based on DBB is established; the transformation of rotary axis is represented by HTM. And lastly, a measuring experiment according to the established identification model is conducted on rotary axes of a five-axis gantry-type milling machine tool. The rest of this paper is arranged as follows: In Section 2, mapping relationships among kinematic errors, geometric profile errors, and tolerances of rotary axes are determined, and kinematic error prediction models are established based on it. In Section 3, identification models of kinematic errors for one type five-axis machine tools' rotary axes based on DBB are established. In Section 4, a verification experiment is presented. And finally, some conclusions are drawn in Section 5.

Table 1 Geometric error parameters

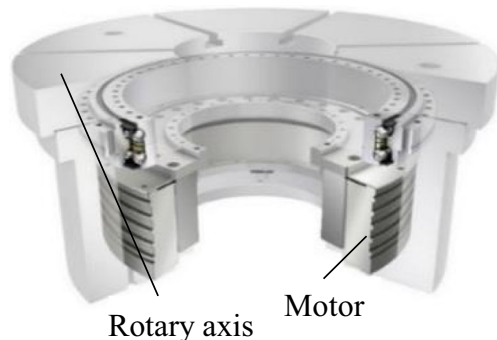|	Axis	Linear error	Angular error	Angular positioning error
PDGEs	B	$\delta_x(b)$	$\varepsilon_x(b)$	$\varepsilon_y(b)$
		$\delta_y(b)$	$\varepsilon_z(b)$	
		$\delta_z(b)$		
	C	$\delta_x(c)$	$\varepsilon_x(c)$	$\varepsilon_z(c)$
		$\delta_y(c)$	$\varepsilon_y(c)$	
		$\delta_z(c)$		
PIGEs	ε_{xc}, ε_{yc}, ε_{xb} and, ε_{bz}			

Fig. 5 Internal structure diagram of rotary axis
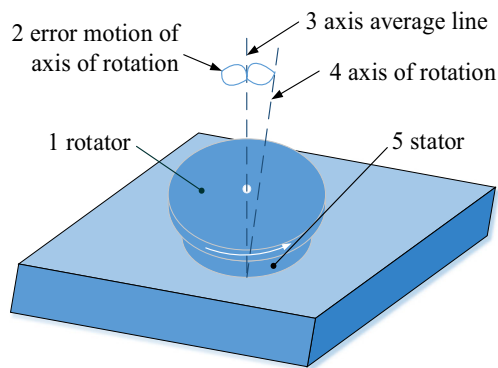
Fig. 6 Error motion diagram of rotary axis

2 Positioning error modeling

2.1 Error components definition

Figure 1 shows the five-axis machine tool studied in this paper, which consists of machine bed (body 1) where workpiece placed on, X-axis slide carriage (body 2), Y-axis slide carriage (body 3), Z-axis slide carriage (body 4), C-axis (body 5), and B-axis (body 6). According to the notation of an axis movement standardized in [30], there are 3 linear axes, X-, Y-, and Z-axis that could be notated in X, Y, and Z, respectively, and 2 rotary axes B- and C-axis simplified in B and C which rotate around Y and Z separately. All of the abovementioned components are seen as rigid bodies in this research. The chosen machine tool is in serial kinematic structure, and could be described in WFXYZCBT from work-piece to tool based on the notation of Schwerd [31]. W denotes work-piece, T denotes tool, and F denotes machine bed. The characteristic of serial structures is that all axes can be moved independently [7]. In this study, the rotary axes are extracted for further research; the specific is shown in Fig. 2.
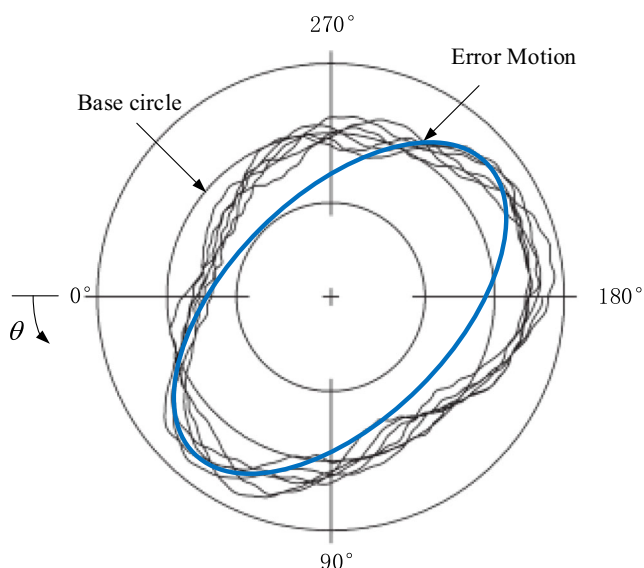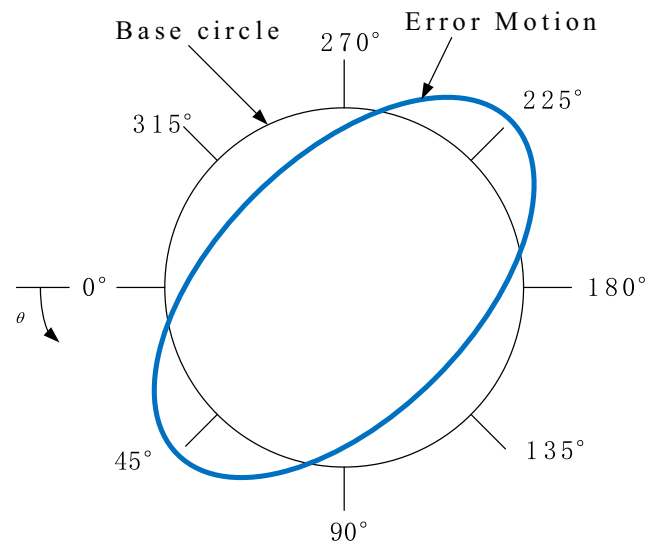

Fig. 7 Total error motion polar plot

Fig. 8 First order of error motion polar plot

According to ISO 230-7 [32], geometric errors are categorized as position independent geometric errors (PIGEs) and position dependent geometric errors (PDGEs), where "position" refers to the command for a controlled axis [11]. PIGEs are introduced in the assembly process and constant regardless of the position of the axis, while PDGEs change with motion and mainly result from the imperfections in components [6]; therefore, they are also mentioned as location errors and kinematic errors [31]. Taking C rotary axis as an instance, its schematic diagram of PIGEs in the C-axis reference coordinate is shown in Fig. 3, where ε_{xC}, ε_{yC} represent the verticality error of between X, Y-axis, and C rotary axis separately. Based on rigid body motion theory, there are six inherent component error parameters of a rotary axis [14]; thus, each moving axis of machine tool has six PDGEs. Figure 4 shows six PDGEs of C-axis, where $\delta_i(C)$ and $\varepsilon_i(C)$ ($i = x, y, z$) represent the linear errors and the angular errors of C-axis along the i direction separately. For a five-axis machine tool, classifying into 3 linear errors, 2 angular errors, and 1 angular positioning error. All geometric error parameters of B- and C-axis are listed in Table 1.
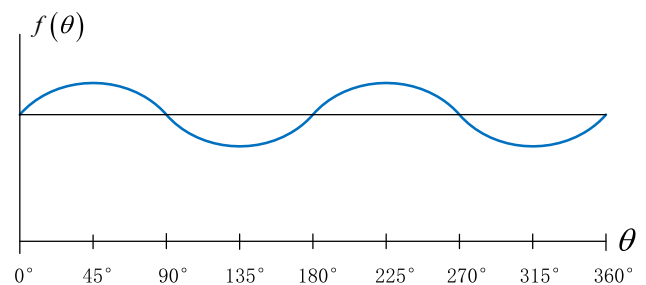

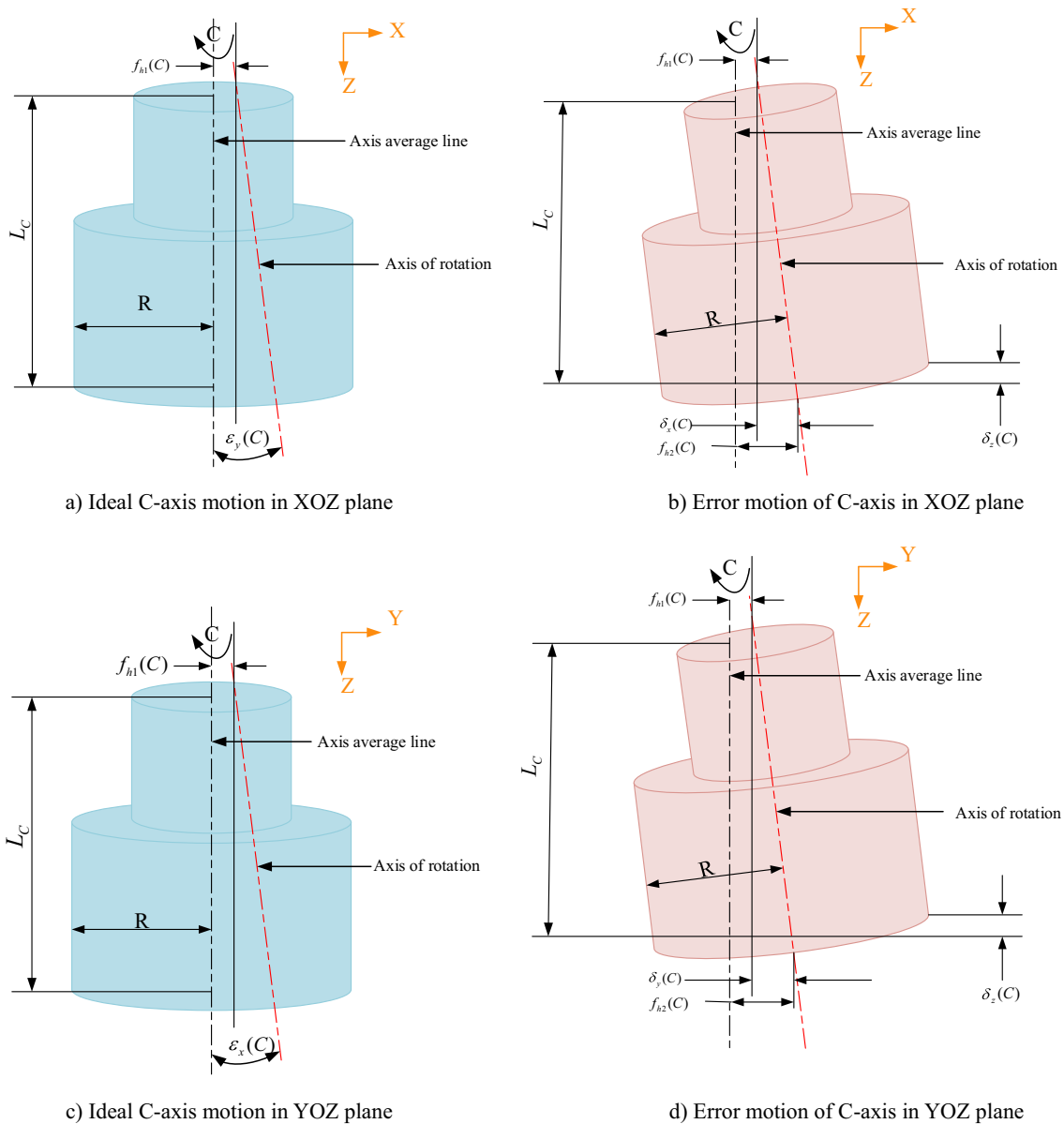**Fig. 9** Rectilinear plot of error motion

a) Ideal C-axis motion in XOZ plane

b) Error motion of C-axis in XOZ plane

c) Ideal C-axis motion in YOZ plane

d) Error motion of C-axis in YOZ plane

Fig. 10 Schematic diagram of C-axis error motion

2.2 Kinematic error prediction model of rotary axis based on tolerance

Rotary axes' kinematic errors are resulted from manufacturing deviation of their geometric profile errors. Specifically, according to [33], error motions of rotary axes are physically caused by 2 factors: non-round bearing surfaces and interaction between supporting structure/bearings and internal or external excitations. Figure 5 shows the internal structure of rotary axis, and Fig. 6 shows the rotary motion considering errors. In conjunction with the abovementioned, there are some relationships between the kinematic errors of rotary axes and their geometric profile errors. In the design stage, geometric profile errors of key components are expressed as tolerances, whose values are known. Consequently, the mapping relationship between kinematic error and tolerance is able to be established via rotary axes' geometric profile errors as a tie, and geometric errors would be predicted based on tolerances.

2.2.1 Mapping relationship between tolerance and geometric error

According to [33], a typical case of error motion is shown as Fig. 7, Fourier series is suitable to express the error motion of rotary axes as Eq. (1) shown, where T denotes the tolerance of rotary motion error, θ denotes the rotary angle, and λ denotes the period of revolution. With the increase of the term of Fourier series, the amplitude of each harmonic constituent gradually decreases; therefore, the influence of geometric profile errors on kinematic errors of rotary axis will decrease as
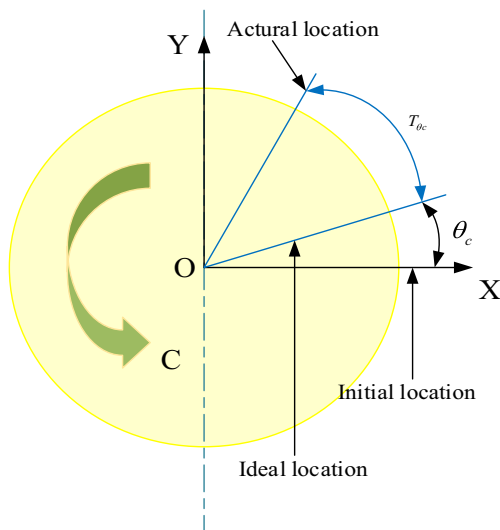
Fig. 11 Schematic diagram of rotary error motion of C-axis

Fig. 13 Structure of double ball-bar

well. This paper aimed at a type of mill high precision milling machine tool whose first term of Fourier series with the largest wavelength has a significant influence on the error motion of rotary axis as well as could express the error motion generally as Fig. 8 shown [33]. Thus, the fundamental error motion, which is the sinusoidal portion of the total error motion that occurs at the rotation frequency, is selected to replace the whole complexed error motion. In addition, it could be observed that the essence of rotary axes' motion is a cyclic motion with period 2π [2]; the error motion of rotary axis in Cartesian coordinate system could be illustrated as Fig. 9; $f(\theta)$ denotes the error motion of rotary axis. Overall, a general mapping model of tolerance and error motion profile of rotary axes could be gotten as Eq. (2) shown.

$$f(\theta) = T \sum_{n=1,3,5...}^{\infty} \frac{1}{n} \sin\left(\frac{2\pi n\theta}{\lambda}\right) \qquad (1)$$

$$f(\theta) = T\sin(\theta) \qquad (2)$$

2.2.2 Mapping relationship between geometric profile error and geometric error

This part, it takes C-axis, which is installed in two borings of the stator, as an instance. Figure 10 shows error motion of C-axis, $f_{h1}(C)$ and $f_{h2}(C)$ denotes error appearance between up-boring and down-boring to match surface of C-axis,
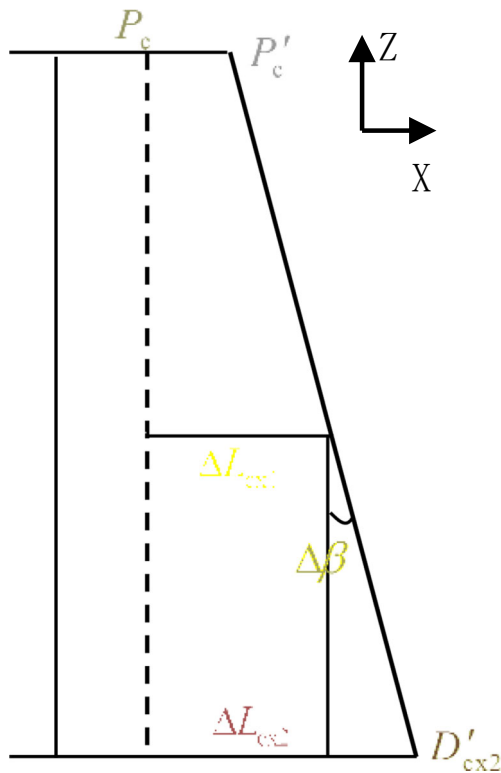
Fig. 12 Unfolding schematic diagram of rotary error motion

Fig. 14 Mechanism of error generation of C-X detection mode

respectively; L_C denotes the length of C-axis, and R denotes the radius of C-axis lower end face.

According to the geometric relationship between error appearance and geometric errors which is shown in Fig. 10, the mapping relationships between geometric profile errors and geometric errors of rotary axes are as following:

$$\delta_x(C) = f_{h2}(C) - f_{h1}(C) \tag{3}$$

$$\varepsilon_y(C) = \frac{\delta_x(C)}{L_C} = \frac{f_{h2}(C) - f_{h1}(C)}{L_C} \tag{4}$$

$$\delta_y(C) = f_{h2}(C) - f_{h1}(C) \tag{5}$$

$$\varepsilon_x(C) = \frac{\delta_y(C)}{L_C} = \frac{f_{h2}(C) - f_{h1}(C)}{L_C} \tag{6}$$

$$\delta_z(C) = R \times \varepsilon_y(C) = \frac{R(f_{h2}(C) - f_{h1}(C))}{L_C} \tag{7}$$

2.2.3 Mapping relationship between tolerance and geometric error

For translational axes, the position errors are represented by cumulative-lead error of screw which could be divided into lead deviation and the cumulative representative lead error. [26]. While as Fig. 11 shown, when it comes to rotary axis, the position error is commonly seen as a whole. Commanding C-axis rotate θ_c, the actual location is deviated from the ideal location, and the value of deviation is represented as $T_{\theta c}$. The specific condition of error motion is depicted as Fig. 12, sinusoidal curve is utilized to fit the various deviation as variable $f_z(C)$, and the rotary error motion could be expressed as Eq. (8).

$$\varepsilon_z(C) = f_z(C) \tag{8}$$

By Eq. (2) to Eq. (8), the mapping mathematical model between tolerance and geometric errors of rotary axis could

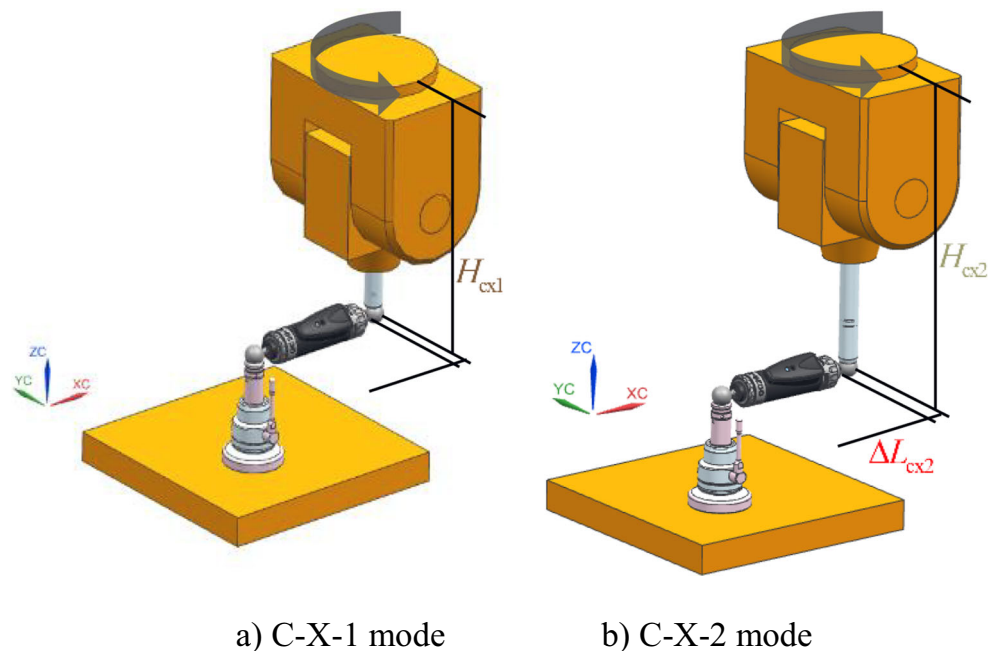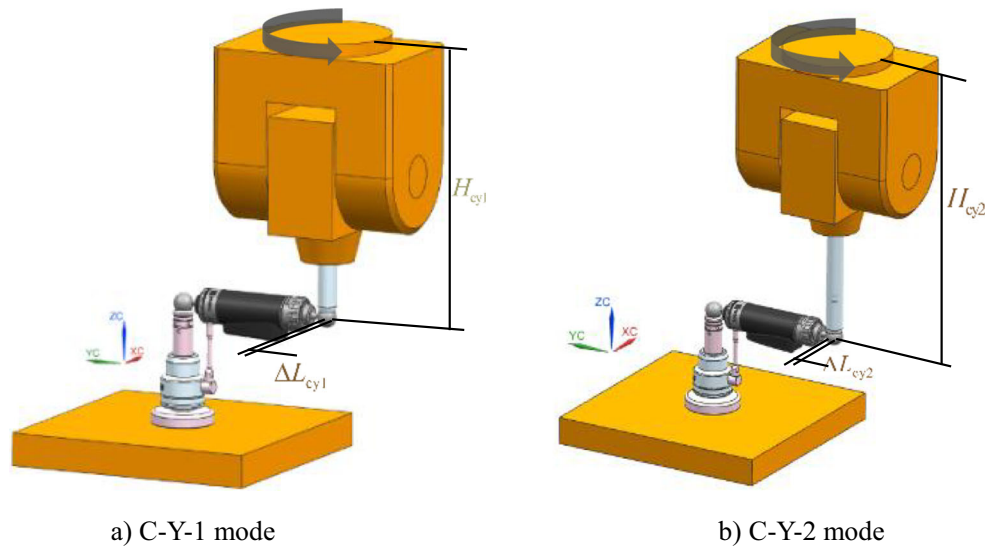Fig. 15 Schematic diagram of error detection method of C-X mode

a) C-X-1 mode   b) C-X-2 mode

Fig. 16 Schematic diagram of error detection method of C-Y mode

a) C-Y-1 mode   b) C-Y-2 mode

be gotten as Eq. (9) to Eq. (14). T_{h1} denotes the tolerance of error profile of $f_{h1}(C)$, T_{h2} denotes the tolerance of error profile of $f_{h2}(C)$, T_h denotes the tolerance of radial error, and $T_{\theta c}$ denotes the tolerance of rotary error.

$$\delta_x(C) = (T_{h2} - T_{h1})\sin\theta_c = T_h\sin\theta_c \tag{9}$$

$$\delta_y(C) = (T_{h2} - T_{h1})\sin\theta_c = T_h\sin\theta_c \tag{10}$$

$$\delta_z(C) = \frac{R(T_{h2} - T_{h1})}{L_C}\sin\theta_c = \frac{RT_h}{L_C}\sin\theta_c \tag{11}$$

$$\varepsilon_x(C) = \frac{(T_{h2} - T_{h1})}{L_C}\sin\theta_c = \frac{T_h}{L_C}\sin\theta_c \tag{12}$$

$$\varepsilon_y(C) = \frac{(T_{h2} - T_{h1})}{L_C}\sin\theta_c = \frac{T_h}{L_C}\sin\theta_c \tag{13}$$

$$\varepsilon_Z(C) = T_{\theta c}\sin\theta_c \tag{14}$$

3 The measurement and identification of geometric error of rotary axes

3.1 The measurement principle based on DBB

DBB measurement system, as shown in Fig. 13, is a precise instrument which is utilized to investigate geometric errors of rotary axes in this study. There are 2 sockets within a DBB measurement system. Socket 1 is clamped by the tool holder on the spindle, another one, Socket 2, is set on the workbench. Two balls of the DBB, Ball 1 and Ball 2, are installed in ball bowls of two sockets, respectively. The measurement of the rotary axes is realized by the high-precision sensor of DBB measurement system that is able to test the displacement deviation between two balls' center positions (Fig. 14).
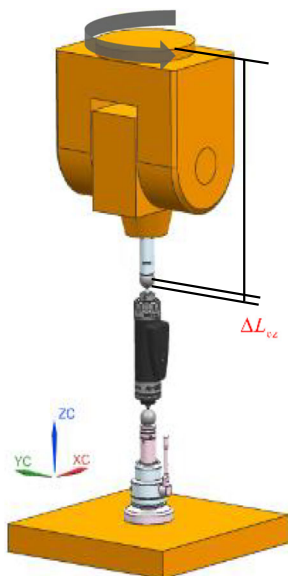

Fig. 17 Schematic diagram of error detection method of C-Z mode

Fig. 18 Initial installation of DBB measurement system

Table 2　QC20-W DBB system performance indicators

Index items	Parameters
Sensor resolution	0.1 μm
Measurement accuracy	± (0.7 + 0.3%L)μm
Measurement range	± 1.0 mm
Sensor stroke	1.25 to + 1.75 mm
Maximum sampling frequency	1000 Hz
Operating temperature	0–40 °C

According to Section 2, there are 12 kinematic error parameters that are needed to be identified, including 6 linear errors ($\delta_x(b)$, $\delta_y(b)$, $\delta_z(b)$, $\delta_x(c)$, $\delta_y(c)$, $\delta_z(c)$), 4 angular errors ($\varepsilon_x(b)$, $\varepsilon_z(b)$, $\varepsilon_x(c)$, $\varepsilon_y(c)$), and 2 angular positioning errors ($\varepsilon_y(b)$, $\varepsilon_z(c)$). Two angular positioning errors ($\varepsilon_y(b)$, $\varepsilon_z(c)$) could be directly tested by the calibration device Renishaw XR20-W without identification. Thus, there are 10 geometric errors of rotary axis that are required to be indirectly identified by DBB. In this paper, C-axis is taken as an example to illustrate the DBB identification.

3.2 Kinematic error identification model based on HTM

When it comes to identify geometric errors of C-axis, follow steps below: test errors in X-Z, Y-Z, and X-Y plane, respectively, which are also called C-X mode, C-Y mode, and C-Z mode separately. The transformations of C-axis are represented by 4 × 4 HTMs.

3.2.1 C-X mode

Under this test mode, adjust the rotary angle of C-axis and B-axis to 0°, parallel the double ball-bar and the X axis of the machine tool, then rotate C-axis and test the variation in X direction. The projection of X-Z plane is shown in Fig. 13, while P_c and P_c' denote ideal and real coordinate origin of C-axis in X-Z plane, respectively, $\triangle x$ denotes the positioning error of C-axis in X direction, $\triangle \beta$ denotes angular error of C-axis in X-Z plane, D_{cx1} and D'_{cx1} denote the ideal and the real position of ball 1 in C-axis coordinate, and H_{cx1} denotes the theoretical distance between P_c to D_{cx1} which is under the

Table 3　C-axis measurement parameters

Parameter	Value
H_{c1}	790 mm
H_{c2}	890 mm
Rotation range	− 90° to + 270°
Sampling frequency	5°

mode C-X-1 as shown in Fig. 15a. As far as D_{cx2}, D'_{cx2}, and H_{cx2}, they denotes the ideal position, actual position, and theoretical distance between D_{cx2} and H_{cx2} separately under C-X-2 mode as shown in Fig. 15b.

$\boldsymbol{D}_c$ is ball 1's ideal position in C-axis coordinate system during the process of C-axis rotating, c denotes the rotary angle of C-axis, H_c denotes the distance between $\boldsymbol{D}_c$ to P_c in general, and H_{cx1} and H_{cx2} are given value of H_c in C-X-1 mode and C-X-2 mode, respectively. $\boldsymbol{D}_c$ could be expressed by Eq. (15). The expansion form is as Eq. (16). $\boldsymbol{D'}_c$, the practical position of the ball 1, would be calculated by Eq. (17), and could be arranged as Eq. (19). The variation of bar in X direction could be computed via Eq. (16) and Eq. (18), and the computed results are as Eq. (19) and Eq. (20).

$$\boldsymbol{D}_c = \begin{bmatrix} \cos(c) & -\sin(c) & 0 & 0 \\ \sin(c) & \cos(c) & 0 & 0 \\ 0 & 0 & 1 & 0 \\ 0 & 0 & 0 & 1 \end{bmatrix} \begin{bmatrix} 0 \\ 0 \\ -H_c \\ 1 \end{bmatrix} \tag{15}$$

$$\boldsymbol{D}_c = \begin{bmatrix} 0 \\ 0 \\ -H_c \end{bmatrix} \tag{16}$$

$$\boldsymbol{D'}_c = \begin{bmatrix} 1 & 0 & \varepsilon_{xc} & 0 \\ 1 & 1 & -\varepsilon_{yc} & 0 \\ -\varepsilon_{xc} & \varepsilon_{xc} & 1 & 0 \\ 0 & 0 & 0 & 1 \end{bmatrix} \begin{bmatrix} \cos(c) & -\sin(c) & 0 & 0 \\ \sin(c) & \cos(c) & 0 & 0 \\ 0 & 0 & 1 & 0 \\ 0 & 0 & 0 & 1 \end{bmatrix}$$
$$\begin{bmatrix} 1 & -\varepsilon_z(C) & \varepsilon_y(C) & \delta_x(c) \\ \varepsilon_z(C) & 1 & -\varepsilon_x(C) & \delta_y(c) \\ -\varepsilon_y(C) & -\varepsilon_x(C) & 1 & \delta_z(c) \\ 0 & 0 & 0 & 1 \end{bmatrix} \begin{bmatrix} 1 & -\varepsilon_{bz} & 0 & 0 \\ \varepsilon_{bz} & 1 & -\varepsilon_{xb} & 0 \\ 0 & \varepsilon_{xb} & 1 & 0 \\ 0 & 0 & 0 & 1 \end{bmatrix} \begin{bmatrix} 0 \\ 0 \\ -H_c \\ 1 \end{bmatrix} \tag{17}$$

$$D'_{cx} = \cos(c)\delta_x(c) - \sin(c)\delta_y(c) - H_c\cos(c)\varepsilon_y(c)$$
$$- H_c\sin(c)\varepsilon_x(c) - H_c\varepsilon_{xc} - H_c\sin(c)\varepsilon_{bz}$$
$$D'_{cy} = \cos(c)\delta_x(c) + \sin(c)\delta_x(c) + H_c\cos(c)\varepsilon_x(c) \tag{18}$$
$$- H_c\sin(c)\varepsilon_y(c) + H_c\varepsilon_{yc} + H_c\cos(c)\varepsilon_{bz}$$
$$D'_{cz} = \delta_z(c) - H_c$$

$$\Delta L_{cx} = D'_{cx} - D_{cx}$$
$$= \cos(c)\delta_x(c) - \sin(c)\delta_y(c) - H_c\cos(c)\varepsilon_y(c) \tag{19}$$
$$- H_c\sin(c)\varepsilon_x(c) - H_c\varepsilon_{xc} - H_c\sin(c)\varepsilon_{bz}$$

$$\cos(c)\delta_x(c) - \sin(c)\delta_y(c) - H_c\cos(c)\varepsilon_y(c) - H_c\sin(c)\varepsilon_x(c)$$
$$= \Delta L_{cx} + H_c\varepsilon_{xc} + H_c\sin(c)\varepsilon_{bz} \tag{20}$$

Obviously, acoording to Eq. (20), different values of the variation of bar, $\triangle L_{cx1}$ and $\triangle L_{cx2}$, would get through changing the distance between ball 1 and the origin coordinate system of C-axis. There are 4 terms without solution as seen in Eq. (21); however, the rand of the coefficient matrix is 2 merely, other terms still need to be solved.

$$\begin{bmatrix} \cos(c) & -\sin(c) & -H_{c1}\cos(c) & H_{c1}\sin(c) \\ \cos(c) & -\sin(c) & -H_{c2}\cos(c) & H_{c2}\sin(c) \end{bmatrix} \begin{bmatrix} \delta_x(c) \\ \delta_y(c) \\ \varepsilon_y(c) \\ \varepsilon_x(c) \end{bmatrix}$$
$$= \begin{bmatrix} \Delta L_{cx1} + H_{c1}\varepsilon_{xc} + H_{c1}\sin(c)\varepsilon_{bz} \\ \Delta L_{cx2} + H_{c2}\varepsilon_{xc} + H_{c2}\sin(c)\varepsilon_{bz} \end{bmatrix} \tag{21}$$
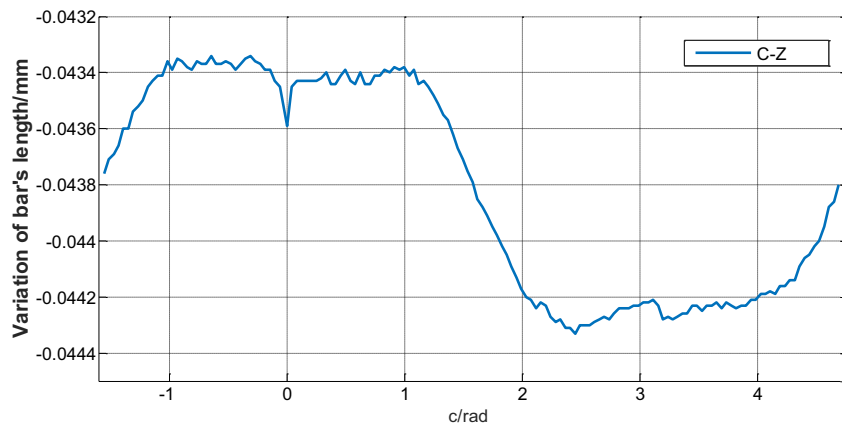
Fig. 19 Direct measurement results of DBB
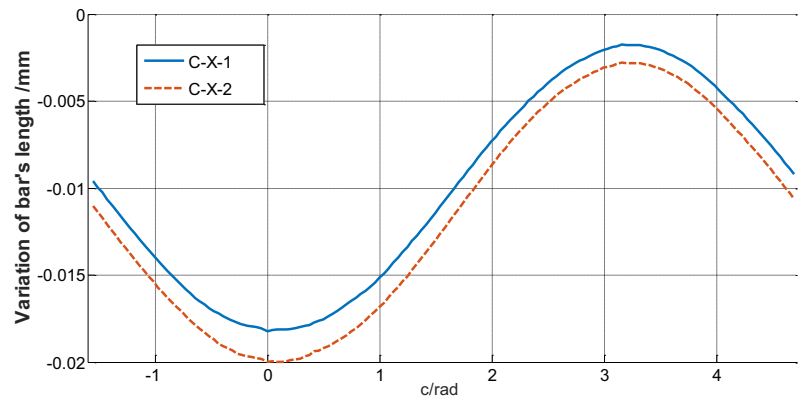
(a) The error measurement curve in C-X mode
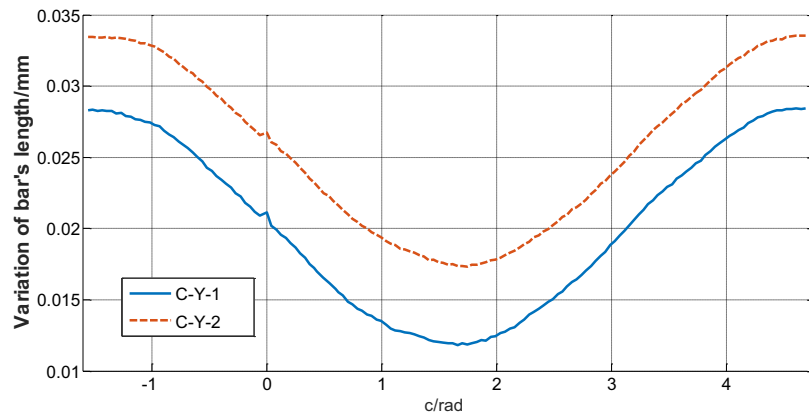
(b) The error measurement curve in C-Y mode

(c) The error measurement curve in C-Z mode

3.2.2 C-Y mode

There are two sub-mode in mode C-Y as shown in Fig. 16. Under this mode, based on the similar principle as C-X mode, keep the angle of B-axis and C-axis in 0°, paralell the Y-axis and machine tool, then rotate C-axis and test the variation of the bar's length in Y direction. In the sub-mode 1, C-Y-1 mode, D_{cy1} denotes the ideal

position of ball 1, and H_{cy1} denotes the theoretical distance between P_c and D_{cy1}, while D'_{cy1} denotes the actual situation. Under the C-Y-2 mode, D_{cy2} denotes the ideal position of ball 1 in another angle, H_{cy2} denotes the theoretical distance between P_c and H_{c2}, and D'_{cy2} denotes the real situation.

The variation of bar's length in Y direction could be calculated via Eq. (16) and Eq. (18), as Eq. (22)

expressed. In this Equation, the parameters ε_{yc}, ε_{bz} are given; therefore, the variation of the length of bar 1 could be simplified as Eq. (23). Similar to C-X mode's process, combining Eq. (21) and Eq. (23) to get Eq. (24). It is obvious that the matrix is non-singular; thus, the 4 geometric error parameters of C-axis could be figured out as Eq. (25) to Eq. (28).

$$
\begin{aligned}
\Delta L_{cy} &= D'_{cy} - D_{cy} \\
&= \cos(c)\delta_y(c) + \sin(c)\delta_x(c) + H_c\cos(c)\varepsilon_x(c) \\
&\quad - H_c\sin(c)\varepsilon_y(c) + H_c\varepsilon_{yc} + H_c\cos(c)\varepsilon_{bz}
\end{aligned}
\tag{22}
$$

$$
\begin{aligned}
\cos(c)\delta_y(c) + \sin(c)\delta_x(c) + H_c\cos(c)\varepsilon_x(c) - H_c\sin(c)\varepsilon_y(c) \\
= \Delta L_{cy} - H_c\varepsilon_{yc} - H_c\cos(c)\varepsilon_{bz}
\end{aligned}
\tag{23}
$$

$$
\begin{bmatrix}
\cos(c) & -\sin(c) & -H_{cy1}\cos(c) & H_{cy1}\sin(c) \\
\cos(c) & -\sin(c) & -H_{cy2}\cos(c) & H_{cy2}\sin(c) \\
\sin(c) & \cos(c) & -H_{cy1}\sin(c) & H_{cy1}\cos(c) \\
\sin(c) & \cos(c) & -H_{cy2}\sin(c) & H_{cy2}\cos(c)
\end{bmatrix}
\begin{bmatrix}
\delta_x(c) \\
\delta_y(c) \\
\varepsilon_y(c) \\
\varepsilon_x(c)
\end{bmatrix}
$$
$$
=
\begin{bmatrix}
\Delta L_{cx1} + H_{cy1}\varepsilon_{xc} + H_{cy1}\sin(c)\varepsilon_{bz} \\
\Delta L_{cx2} + H_{cy2}\varepsilon_{xc} + H_{cy2}\sin(c)\varepsilon_{bz} \\
\Delta L_{cy1} + H_{cy1}\varepsilon_{yc} + H_{cy1}\cos(c)\varepsilon_{bz} \\
\Delta L_{cy2} + H_{cy2}\varepsilon_{yc} + H_{cy2}\cos(c)\varepsilon_{bz}
\end{bmatrix}
\tag{24}
$$

$$
\varepsilon_x(c) = \frac{\cos(c)(\Delta L_{cy1} - \Delta L_{cy2}) + \sin(c)(\Delta L_{cx2} - \Delta L_{cx1})}{H_{cy1} - H_{cy2}}
$$
$$
- \cos(c)\varepsilon_{yc} - \sin(c)\varepsilon_{xc} - \varepsilon_{bz}
\tag{25}
$$

$$
\varepsilon_x(c) = \frac{\cos(c)(\Delta L_{cx2} - \Delta L_{cx1}) + \sin(c)(\Delta L_{cy2} - \Delta L_{cy1})}{H_{cy1} - H_{cy2}}
$$
$$
- \cos(c)\varepsilon_{yc} - \sin(c)\varepsilon_{yc}
\tag{26}
$$

$$
\delta_y(c) = \frac{\sin(c)(H_{c2}\Delta L_{cx1} - H_{c1}\Delta L_{cx2}) + \cos(c)(H_{c1}\Delta L_{cy2} - H_{c2}\Delta L_{cy1})}{H_{cy1} - H_{cy2}}
\tag{27}
$$

$$
\delta_x(c) = \frac{\sin(c)(H_{c1}\Delta L_{cx2} - H_{c2}\Delta L_{cx1}) + \sin(c)(H_{c1}\Delta L_{cy2} - H_{c2}\Delta L_{cy1})}{H_{cy1} - H_{cy2}}
\tag{28}
$$

3.2.3 C-Z mode

Lastly, to distinguish the axial aligning errors of C-axis, C-Z mode is proposed as shown in Fig. 17. Adjust B- and C-axis to 0°, paralell the bar and Z-axis, then rotate Z-axis to test the variation of bar in Z direction. Till now, there is only one error parameter that is unknown, thus only one identifying equation

is needed to establish in this mode. D_{cz} denotes the ideal situation of ball 1, and the distance between P_c and D_{cz} is indicated as H_{cz}, the actual situation of ball 1 is indicated as D'_{cz}.

The variation of bar, calculated by Eq. (16) to Eq. (18), is expressed by Eq. (29).

$$
\Delta L_{cz} = D'_{cz} - D_{cz} = \delta_z(c)
\tag{29}
$$

So far, 5 geometric errors of C-axis have been identified totally.

4 Experimental verification

In order to validate the feasibility, accuracy, and effectiveness of the proposed approach of predicting rotary axes' kinematic, experiments are conducted on a gantry-type milling machine tools. A DBB system, QC20-W provided by Renishaw, is utilized in this experiment, and the main parameters are shown in Table 1. The installation of DBB is shown in Fig. 15. Before measuring, the machine tool is warmed up for 20 min according to the standard procedure [34], and in order to minimize the impact of thermal error, the ambient temperature is controlled within 20 ± 2 °C [18]. What is more, for eliminating the influence of three translational axes, geometric errors of linear axes are measured and compensated to be significantly small and can be neglected [35]. Moreover, the test was repeated until the repeatability was within the tolerance to guarantee the measurement stability, averages, and standard deviations of all testing results that are calculated based on the repeatability tests Fig. 18.

Kinematic errors of rotary axes are tested based on the identification method which is presented in Section 3. Take C-axis as an instance, the relative parameters of the test experiment is listed in Tables 2 and 3. The error measurement curve in C-X, Y, and Z mode, which indicate the relationship between rotary angle and variation of DBB, is shown in Fig. 19.

Finally, bring the measurement values of bar's length into identification model to obtain identification points based on the proposed identification method in Section 3, at the same time, bring the factory and tolerance parameters of the machine tool provided by the manufacturer into Eq. (9) to Eq. (14), then analyze the fitting of identification points and prediction model curves, the mathematical expressions of geometric error prediction model of C-axis are listed in the second column of Table 5. The comparison results of prediction model and measurement result is shown in Fig. 20.

From Fig. 20, it can be seen that the minimum and maximum identified position error value of C-axis are − 13.6 μm and 32.7 μm, respectively, which means the range of the

(a) Angular positioning error of C-axis

(c) The radial error in Y-direction of C-axis

(b) The radial error in X-direction of C-axis

(d) The axial error in Z-direction of C-axis

(e) The angle error around X-axis of C-axis

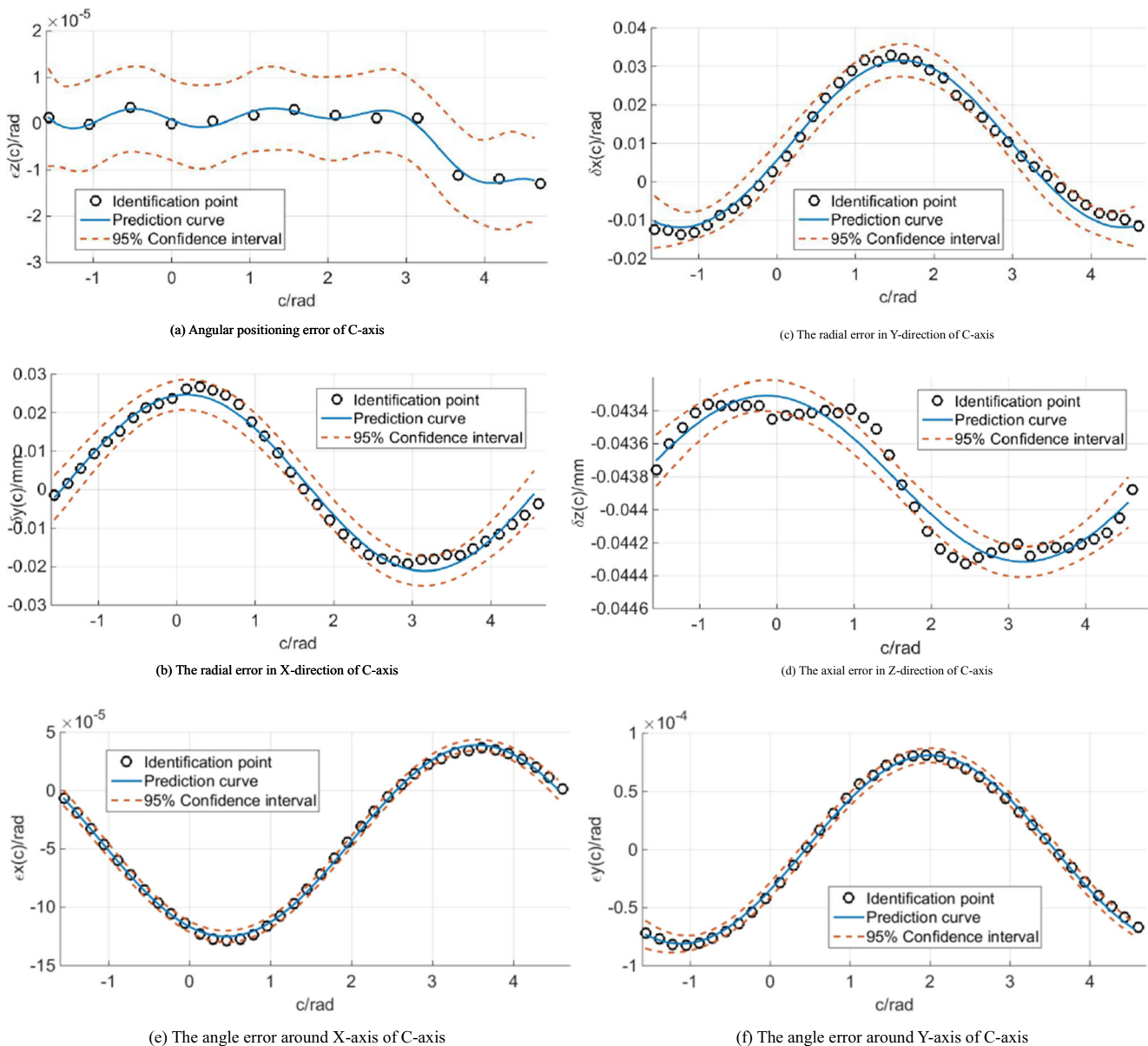(f) The angle error around Y-axis of C-axis

Fig. 20 Comparisons between identification result and prediction model of C-axis geometric errors

identified position error $\delta_x(c)_i$ is 46.3 μm; and the minimum and maximum predicted position error value of C-axis are −11.7 μm and −31.9 μm, respectively, which means the range of the predicted position error $\delta_x(c)_p$ is 43.6 μm. The difference value between the range of measured result and predicted result is 2.7 μm. Similarly, the range of the measured and predicted results, and difference values of other kinematic errors can be obtained, as shown in Table 4.

Different values may be caused by two primary causes, (1) the existence of non-geometric error sources, such as control errors, dynamitic errors, assembly inaccuracy, and thermal errors; and (2) some assumptions were utilized for predicting kinematic errors.

Obviously, most of the measurement points are within the confidence interval of prediction model. After further quantification, the evaluation indexes of C-axis prediction model is shown in the third and fourth column of Table 5, where SSE denotes residual sum of squares between estimated value and identified point, R^2 denotes fitting equation's coefficient of determination. The quantitative analysis result shows that, the presented predicting model is able to reflect the motion laws of C-axis kinematic errors. The proposed geometric error prediction method of rotary axes makes it possible for further guiding early accuracy design of multi-axis machine tools.

Table 4 The range of predicted and measured values of kinematic errors

	$\delta_x(c)/\mu m$	$\delta_y(c)/\mu m$	$\delta_z(c)/\mu m$	$\varepsilon_x(c)/\mu rad$	$\varepsilon_y(c)/\mu rad$	$\varepsilon_y(c)/\mu rad$
Identified	46.3000	46.2000	0.9100	0.16745	0.1608	0.0517
Predicted	43.6000	45.5000	1.0100	0.16600	0.1600	0.0500
Difference value	2.7000	0.7000	0.1000	0.00145	0.0008	0.0017

5 Conclusion

This paper proposes a novel geometric errors predicting method of five-axis machine tools' rotary axes, based on tolerance. The key in this method is that it takes geometric profile error as a bridge to link geometric error and tolerance. Compared with previous researches, there are some following advantages of this new approach:

(1) Consider geometric errors in more fundamental level and take into account the basic factors, geometric profile errors, and tolerances of key components. Therefore, the established kinematic error model is satisfied with the structural feature of rotary axis.
(2) According to the structural feature, the periodic variation regulation of rotary axis kinematic errors is calculated by Fourier series function and expressed by tolerances. It realizes that predict kinematic errors of rotary axes in design stage.
(3) In consideration of the dynamic characteristic of rotary axes', kinematic errors establish a more practical identifying model of rotary axes based on DBB.

To verify the effectiveness of the presented method, a measuring experiment is conducted. The SEE and R^2 could be calculated according to experimental identifying results and predicting model, the SSE of $\varepsilon_z(c)$, $\delta_x(c)$, $\varepsilon_y(c)$, $\delta_z(c)$, $\varepsilon_x(c)$, and $\delta_y(c)$ are 7.7716×10^{-11}, 1.2064×10^{-4}, 2.7838×10^{-10}, 2.9639×10^{-7}, 1.8966×10^{-10}, and 2.7838×10^{-10}, respectively; and the R^2 are 0.8978, 0.9876, 0.9978, 0.9453, 0.9985, and 0.9978, respectively. The experimental results show that the predicted models of rotary axes' kinematic errors are in coincidence with the measured results basically, little residual errors are able to be neglect. Hence, there is no doubt that the approach is reliable and effective for predicting geometric errors of rotary axes in a five-axis machine tool. Furthermore, this method is universal, and could be extended to other configurations of five-axis machine tools as well.

Despite the progress made in this work, only the first order of Fourier series is selected to be used; consequently, there is a space to shrink the error remainder. In further researches, there would be more orders taken into account to improve the accuracy of prediction. In addition, the prediction effect of C-axis vertical positioning error, $\delta_z(c)$ whose R^2 is 0.9453, is not accuracy enough compared with another 5 items of the geometric error parameters, therefore needed to be further improved in the future as well.

Table 5 Geometric error prediction models of C-axis and the assessment

Geometric error	Prediction model	SSE	R^2
$\delta_x(c)$	$\delta_x(c) = 0.0217 \ \sin(1.1131c - 0.1963) + 0.0099$	1.2064×10^{-4}	0.9876
$\delta_y(c)$	$\delta_y(c) = 0.0230 \ \sin(1.0354c - 1.4450) + 0.0018$	1.2337×10^{-7}	0.9873
$\delta_z(c)$	$\delta_z(c) = 5.0416 \times 10^{-4} \ \sin(0.9446c - 1.6969) + 0.0438$	2.9639×10^{-7}	0.9453
$\varepsilon_x(c)$	$\varepsilon_x(c) = 8.2181 \times 10^{-5} \ \sin(1.0115c - 1.1161) + 4.3092 \times 10^{-5}$	1.8966×10^{-10}	0.9985
$\varepsilon_y(c)$	$\varepsilon_y(c) = 8.1000 \times 10^{-5} \ \sin(1.007c - 0.4419) + 8.3066 \times 10^{-9}$	2.7838×10^{-10}	0.9978
$\varepsilon_z(c)$		1.0650×10^{-11}	0.9753

$$\varepsilon_z(c) = 6.2025 \times 10^{-5} \sin\left(\frac{0.1832c}{2} + 3.0467\right)$$
$$+ 1.0194 \times 10^{-5} \sin\left(\frac{1.4799c}{2} + 0.5737\right)$$
$$+ 3.2155 \times 10^{-5} \sin\left(\frac{6.2908c}{2} + 0.9113\right)$$
$$+ 3.3184 \times 10^{-5} \sin\left(\frac{6.2908c}{2} + 2.2898\right)$$

References

1. Bi QZ, Huang ND, Sun C, Wang YH, Zhu LM, Ding H (2015) Identification and compensation of geometric errors of rotary axes on five-axis machine by on-machine measurement. Int J Mach Tools Manuf 89:182–191. https://doi.org/10.1016/j.ijmachtools.2014.11.008

2. Nojehdeh MV, Arezoo B (2016) Functional accuracy investigation of work-holding rotary axes in five-axis CNC machine tools. Int J Mach Tools Manuf 111:17–30. https://doi.org/10.1016/j.ijmachtools.2016.09.002

3. Ma Y (2001) Sensor placement optimization for thermal error compensation on machine tools [D]. University of Michigan, Ann Arbor

4. Li H, Li YG, Mou WP, Hao XZ, Li ZX, Jin Y (2017) Sculptured surface-oriented machining error synthesis modeling for five-axis machine tool accuracy design optimization. Int J Adv Manuf Technol 89:3285–3298. https://doi.org/10.1007/s00170-016-9285-x

5. Fu GQ, Fu JZ, Xu YT, Chen ZC, Lai JT (2015) Accuracy enhancement of five-axis machine tool based on differential motion matrix: geometric error modeling, identification and compensation. Int J Mach Tools Manuf 89:170–181. https://doi.org/10.1016/j.ijmachtools.2014.11.005

6. Lee K, Yang SH (2013) Measurement and verification of position-independent geometric errors of a five-axis machine tool using a double ball-bar. Int J Mach Tools Manuf 70:45–52. https://doi.org/10.1016/j.ijmachtools.2013.03.010

7. Schwenke H, Knapp W, Haitjema H, Weckenmann A, Schmitt R, Delbressine F (2008) Geometric error measurement and compensation of machines-an update. CIRP Ann 57:660–675. https://doi.org/10.1016/j.cirp.2008.09.008

8. Lasemi A, Xue DY, Gu PH Accurate identification and compensation of geometric errors of 5-axis CNC machine tools using double ball bar. Meas Sci Technol 27:055004(18pp). https://doi.org/10.1088/0957-0233/27/5/055004

9. Chen GD, Liang YC, Sun YZ (2013) Volumetric error modeling and sensitivity analysis for designing a five-axis ultra-precision machine tool. Int J Adv Manuf Technol 68:2525–2534. https://doi.org/10.1007/s00170-013-4874-4

10. Ramesh R, Mannan MA, Poo AN (2000) Error compensation in machine tools—a review: Part I: geometric, cutting-force induced and fixture-dependent errors. Int J Mach Tools Manuf 40:1235–1256. https://doi.org/10.1016/S0890-6955(00)00009-2

11. JiangXG CRJ (2015) A method of testing position independent geometric errors in rotary axes of a five-axis machine tool using a double ball bar. Int J Mach Tools Manuf 89:151–158. https://doi.org/10.1016/j.ijmachtools.2014.10.010

12. Lei WT, Wang WC, Fang TC (2014) Ballbar dynamic tests for rotary axes of five-axis CNC machine tools. Int J Mach Tools Manuf 82-83:29–41. https://doi.org/10.1016/j.ijmachtools.2014.03.008

13. Ding S, Huang XD, Yu CJ, Wang W (2016) Actual inverse kinematics for position-independent and position-dependent geometric error compensation of five-axis machine tools. Int J Mach Tools Manuf 111:55–62. https://doi.org/10.1016/j.ijmachtools.2016.10.001

14. He ZY, Fu JZ, Zhang LC, Yao XH (2015) A new error measurement method to identify all six error parameters of a rotational axis of a machine tool. Int J Mach Tools Manuf 88:1–8. https://doi.org/10.1016/j.ijmachtools.2014.07.009

15. Xiang ST, Yang JG, Zhang Y (2014) Using a double ball bar to identify position-independent geometric errors on the rotary axes of five-axis machine tools. Int J Adv Manuf Technol 70:2071–2082. https://doi.org/10.1007/s00170-013-5432-9

16. Xia HJ, Peng WC, Ouyang XB, Chen XD, Wang SJ, Chen X (2017) Identification of geometric errors of rotary axis on multi-axis machine tool based on kinematic analysis method using double ball bar. Int J Mach Tools Manuf 122:161–175. https://doi.org/10.1016/j.ijmachtools.2017.07.006

17. Abbaszadeh-Mir Y, Mayer JRR, Cloutier G, Fortin C (2010) Theory and simulation for the identification of the link geometric errors for a five-axis machine tool using a telescoping magnetic ball-bar. Int J Prod Res 40:4781–4797. https://doi.org/10.1080/00207540210164459

18. Qiao Y, Chen YP, Yang JX, Chen B (2017) A five-axis geometric errors calibration model based on the common perpendicular line (CPL) transformation using the product of exponentials (POE) formula. Int J Mach Tools Manuf 118-119:49–60. https://doi.org/10.1016/j.ijmachtools.2017.04.003

19. Zhang Y, Yang JG, Zhang K (2013) Geometric error measurement and compensation for the rotary table of five-axis machine tool with double ballbar. Int J Adv Manuf Technol 65:275–281. https://doi.org/10.1007/s00170-012-4166-4

20. Chen JX, Lin SW, Zhou XL, Gu TQ (2016) A ballbar test for measurement and identification the comprehensive error of tilt table. Int J Mach Tools Manuf 103:1–12. https://doi.org/10.1016/j.ijmachtools.2015.12.002

21. Jiang L, Ding GF, Li Z, Zhu SW, Qin SF (2012) Geometric error model and measuring method based on worktable for five-axis machine tools. J Eng Manuf 227:32–44. https://doi.org/10.1177/0954405412462944

22. ISO230-2 (2006) Test code for machine tools-Part 2:Determination of accuracy and repeatability of positioning of numerically controlled axes

23. Fu GQ, Fu JZ, Shen HY, Xu YT, Jin YA (2015) Product-of-exponential formulas for precision enhancement of five-axis machine tools via geometric error modeling and compensation. Int J Adv Manuf Technol 81:289–305. https://doi.org/10.1007/s00170-015-7035-0

24. Lu XD, Jamalian A (2011) A new method for characterizing axis of rotation radial error motion: part 1. Two-dimensional radial error motion theory. Precis Eng 35:73–94. https://doi.org/10.1016/j.precisioneng.2010.08.005

25. Wu CJ, Fan JW, Wang QH, Chen DJ (2018) Machining accuracy improvement of non-orthogonal five-axis machine tools by a new iterative compensation methodology based on the relative motion constraint equation. Int J Mach Tools Manuf 124:80–98. https://doi.org/10.1016/j.ijmachtools.2017.07.008

26. Fan JW, Tao HH, Wu CJ, Pan R, Tang YH, Li ZS (2018) Kinematic errors prediction for multi-axis machine tools' guideways based on tolerance. Int J Adv Manuf Technol 98:1131–1144. https://doi.org/10.1007/s00170-018-2335-9

27. Wu CJ, Fan JW, Wang QH, Pan R, Tang YH, Li ZS (2018) Prediction and compensation of geometric error for translational axes in multi-axis machine tools. Int J Adv Manuf Technol 95:3413–3435. https://doi.org/10.1007/s00170-017-1385-8

28. Lee K, Lee DM, Yang SH (2012) Parametric modeling and estimation of geometric errors for a rotary axis using double ball-bar. Int J Adv Manuf Technol 62:741–750. https://doi.org/10.1007/s00170-011-3834-0

29. Ekinci TO, Mayer JRR (2007) Relationships between straightness and angular kinematic errors in machines. Int J Mach Tools Manuf 47:1997–2004. https://doi.org/10.1016/j.ijmachtools.2007.02.002

30. ISO 841 (2001) Industrial automation systems and integration: Numerical control of machines: coordinate system and motion nomenclature

31. Lee K, Yang SH (2013) Robust measurement method and uncertainty analysis for position-independent geometric errors of a rotary axis using a double ball-bar. Int J Precis Eng 14:231–239. https://doi.org/10.1007/s12541-013-0032-z

32. ISO 230-7 (2015) Test code for machine tools-Part 7: geometric accuracy of axes of rotation

33. ANSI/ASME B89.3.4M (1985) Axis of rotation: methods for specifying and testing

34. ISO 230-1 (2012). Test code for machine tools-Part 1: geometric accuracy of machines operating under no-load or quasi-static conditions

35. Chen YT, More P, Liu CS, Cheng CC (2019) Identification and compensation of position-dependent geometric errors of rotary axes on five-axis machine tools by using a touch-trigger probe and there spheres. Int J Adv Manuf Technol 102:3077–3089. https://doi.org/10.1007/s00170-019-03413-x